



Received: 18/02/2024

Accepted: 28/02/2024

Anales de Edificación

Vol. 10, Nº1, 17-24 (2025)

ISSN: 2444-1309

DOI:10.20868/ade.2024.5384

Cálculo de soleras de hormigón para centrales hortofrutícolas y centros logísticos mediante las fórmulas de Westergard modificadas y las de Meyerhof

Calculation of concrete floors for fruit and vegetable processing plants and logistics centres using the modified Westergard and Meyerhof formulae

Esteban Gargallo Tatay^a; Carlos Manuel Ferrer Gisbert^b; Miguel Redón Santafé^b; Juan Bautista Torregrosa Soler^b; Francisco Javier Sánchez Romero^b; José Javier Ferrán Gozávez^b; Pablo Sebastián Ferrer Gisbert^c

¹ Universitat Politècnica de València. Doctorando del Programa en Programa de Diseño, Fabricación y Gestión de Proyectos Industriales. esteban.gargallo.tatay@gmail.com

² Universitat Politècnica de València. D.I.R.A. Unidad de Construcción. jjferran@agf.upv.es; caferrer@agf.upv.es

³ Universitat Politècnica de València. Departamento de Proyectos de Ingeniería; pferrer@dpi.upv.es

Resumen-- En las centrales hortofrutícolas y los centros logísticos de la cadena agroalimentaria, tras una campaña de visitas a múltiples instalaciones de este sector, se ha determinado que los puntos más desfavorables en cuanto a cargas sobre la solera se refieren, son las cargas ocasionadas por los vehículos estibadores y por las estanterías de almacenaje. En la presente ponencia, a partir de los datos obtenidos en dichas visitas, se ha desarrollado un cálculo analítico mediante las fórmulas de Westergaard (TR-34, 1997) y Meyerhof (TR-34, 2014) con objeto de optimizar el diseño de soleras.

Palabras clave— centrales hortofrutícolas; Meyerhof; Westergaard.

Abstract— In the fruit and vegetable plants and logistics centres of the agri-food chain, after a campaign of visits to multiple facilities in this sector, it has been determined that the most unfavourable points in terms of loads on the floor are the loads caused by the dunnage vehicles and by the storage racks. In this paper, based on the data obtained in these visits, an analytical calculation has been developed using the formulae of Westergaard (TR-34, 1997) and Meyerhof (TR-34, 2014) to optimise the design of sills.

Index Terms— Fruit and vegetable plants; Meyerhof; Westergaard.

I. INTRODUCTION

In fruit and vegetable plants, as well as in related logistics centres and any other type of industry, screeds are fundamental construction elements for the proper functioning

of daily activities. A correct design, calculation and installation is necessary to provide the structure with the necessary resistance against wear caused by the movement and storage of goods, as well as resistance to shocks, impacts and fatigue. However, the pressure to reduce project execution costs or the

E. G. T. is PhD student within Industrial Projects Management, Design, and manufacturing PhD program at Universidad Politécnica de Valencia. C. M. F. G., M. R. S., J. B. T. S., F. J. S. R., and J. J. F. G. are associate professors at

Construction department from Universidad Politécnica de Valencia. P. S. F. G. is associate professor at Engineering projects department from Universidad Politécnica de Valencia.

lack of rigor in design can lead to multiple failures of this structural element throughout its useful life, hindering or preventing the development of the daily activities of the industry. All this, together with the scarcity of specific regulations in Spain, compared to other countries (Concrete Society, 2014) (ACI-360, 2010), (Juhasz & Schaul, 2019) mean that this part of the construction projects is in many cases left with a deficient execution that reports problems in the short or medium term.

To find out which are the most important loads to consider in the calculations of screeds in this type of industry, multiple companies in the sector have been visited, allowing us to determine how the most critical points are, the transport of pallets by stevedoring vehicles and the cold storage in racks of unit loads awaiting dispatch. In the same way, in logistics centres related to this type of industry, the storage of clothing materials causes significant loads on this element.

During these visits, on-site measurements are made of the contact areas, both anchor plates of the racks and of the wheels of the stevedoring vehicles with the floor (with and without load) to know the real loads in service that these structures support. The loads acting in the calculation of screeds are values that are a priori unknown (Martini *et al.*, 2020; Serykh *et al.*, 2019), in this way, a better estimation of these stresses allows for better dimensioning (Juhasz *et al.*, 2019; 2019), while considering different types of terrain (Urbonas *et al.*, 2020; Tursikis *et al.*, 2020).

First, the different ballast coefficients have been calculated according to the terrain, for which the multilayer model of Burmister (1943) has been used. It is represented from two or more layers on an infinite massif of the Boussinesq type. This model represents each layer with three fundamental parameters: thickness, modulus of elasticity and modulus of Poisson, which gives each material different elastic properties (see Fig. 1).

These types of warehouses are usually built high above the natural terrain to facilitate the loading and unloading of trucks. Therefore, in the model shown, a soil layer thickness of 65 cm and a gravel layer of 49 cm have been estimated, estimating an upper screed height of 120 cm.

Considering that all materials are homogeneous, isotropic, and linearly elastic, each pavement layer can be represented by three parameters: thickness, modulus of elasticity, and Poisson's coefficient. Each of these layers can have different elastic properties. Likewise, it is considered infinite horizontally, with the lower layer extending infinitely in the vertical direction.

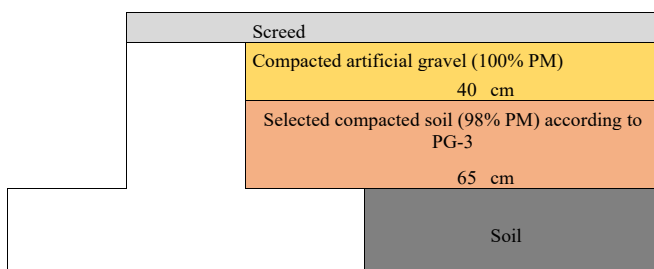


Fig. 1 Burmister Multilayer Model Schematic (Own elaboration)

Using the following expression we can calculate the modulus of deformation of the set:

$$E_s = \frac{n \cdot (n - 1)}{\left[\left(\sum_{i=1}^{n-1} h_i \right) \left(\sum_{i=1}^{n-1} \frac{1}{h_i \cdot E_i} \right) + \frac{n - 1}{E_n} \right]} \quad (1)$$

$$E_{i,zahorra} = 1.000 \frac{kgf}{cm^2} = 98,07 MPa$$

$$E_{i,suelo} = 500 \frac{kgf}{cm^2} = 49,03 MPa$$

To know the behaviour of the different screeds according to the loads applied, 5 distinct types of soil have been considered for the calculation, the characteristics of which are described in Table 1.

With the data presented in Table 1 and using Burmister's model, we can obtain the ballast coefficient in an approximate way by means of the following expression due to Escario (Escario *et al.*, 1973):

$$K_s \cong \frac{E_s}{1,18 \cdot a} \quad (2)$$

Where:

a (cte) = 38,10.

II. METHODS

On the market we can find a wide availability of models of electric counterbalances. The contact area of your wheels is determined by many factors such as: the type of wheel, the weight of the battery and the equipment in general or the maximum load capacity it will be able to support. For this reason, measurements have been taken from the most common forklifts that we can find in fruit and vegetable warehouses. These usually have a nominal capacity between 15kN – 20kN and can vary depending on whether there are specific needs in the warehouse.

To facilitate comprehension and reduce the length of the document, the two models of most widespread use of electric counterbalances in fruit and vegetable plants and related logistics warehouses have been chosen. Specifically, the Toyota 8FBE20 (see Fig. 2) and Toyota 8FBE16 (see Fig. 3) models (Gargallo Tatay *et al.*, 2022). With each of the vehicles studied, two or three measurements were made of the contact surface of the wheel with the screed (Ferrer *et al.*, 2000).

TABLE I
CHARACTERISTICS OF THE SOILS USED IN THE CALCULATIONS.

Soil	Description	E_n (kgf/cm ²)	E_s (kg/cm ²)	k_s (kg/cm ³)
Hard	Hard soil soil (natural gravel)	500	608,780	13,54
Medium/ Hard	Medium soil (hard sands, consolidated clays)	300	479,140	10,66
Medium/ Soft	Medium soil (soft sands, somewhat consolidated clays)	200	378,411	8,42
Soft	Soft Soil	100	232,057	5,16



Fig. 2. Toyota Electric Counterbalance Model 8FBE20 (Own elaboration)

The first of these was conducted with the machine without lifting load, only with its own weight and that of the driver. The second of the measurements, if any, was made at half load and the third of the measurements was made at full load.

The data that can be obtained from the measurements conducted are shown in Table 2.

Similarly, in the case of racking, a 3-height shelving model used in a logistics centre for packaging materials for fruit and vegetable products, owned by a fruit and vegetable exporting



Fig. 3. Toyota Electric Counterbalance Model 8FBE16 (Own elaboration)

company, has been chosen as an example.

In this type of logistics warehouse, responsible for supplying cooperatives with the necessary materials for the manufacture of fruit and vegetable products, we can find pallets with an average weight of 4.61 kN. The anchor plates of the central columns of the racks shown in Fig. 5 can withstand a load of around 55.31 kN.

Table 3 shows some of the characteristics of the shelving under study.



Fig. 4.. Anecoop Logistics Centre S.Coop. (Own elaboration)



Fig. 5. Anecoop S.Coop logistics centre racking. (Own elaboration)

TABLE II
 DATA ON ELECTRIC COUNTERBALANCES.

Model	Contact Length with Applied Load (cm)		Contact Area with Applied Load (cm ²)		Axle load including driver weight (between 75 – 100 kg depending on the case) (kg)		Pressure per wheel (kg/cm ²)	
	R.D.	R.T.	R.D.	R.T.	Front	Back	R.D.	R.T.
Toyota 8FBE20T	16,60	8,41	211,86	118,45	4.805	617	11,34	2,61
Toyota 8FBE16T	15,64	5,92	278,78	82,09	4.151	532	7,45	3,24

Note: (R.) indicates wheel(s); (D.) indicates front/s and (T.) indicates rear/s

TABLE III
CHARACTERISTICS OF THE SHELVING SYSTEM STUDIED.

Plate Size (W x D)	Plate's Area (cm ²)	Nº Columns	Distance between column plates (cm)	Nº Rows	Distance between rows plates (cm)	Nº Levels	Heigh between levels (cm)
12 x14	160	5	173/260	2	91	3	150

A. Theoretical basis

Classical Westergaard expressions have been used for the calculation of stresses due to wheel load (Concrete Society, 1994) (Concrete Society, 2014).

Westergaard started from the following assumptions:

- The concrete slab is a homogeneous, isotropic, and elastic solid
- The load is evenly distributed over a circular contact area
- The reaction of the soil is vertical and proportional to the deformation of the slab. Soil is assumed to be elastic in its vertical component.

Westergaard proposed three formulas that provide the maximum flexural stresses in concrete as a function of the point of application of the load:

- Maximum tensile stress on concrete on the top face of the slab due to a load applied at the corner:

$$\sigma_e = \frac{3 \cdot P}{h^2} \cdot \left[1 - \left(\frac{a \cdot \sqrt{2}}{l} \right)^{1,2} \right] \quad (3)$$

Where:

- a = contact area's radius of the equivalent circle cm²
- h = thickness of the slab in cm
- l = relative stiffness radius

$$l = \left[\frac{E_{cm}}{12} \cdot \frac{h^3}{(1 - \mu^2) \cdot k} \right]^{0,25} \quad (4)$$

- Maximum tensile stress on concrete on the underside of the slab due to a load applied at the edge:

$$\sigma_b = 0,529 \cdot (1 + 0,548 \cdot \mu) \cdot \frac{P}{h^2} \cdot \left[\log \left(\frac{E_{cm} \cdot h^3}{k \cdot r^4} \right) + \log \left(\frac{r}{1 - \mu^2} \right) - 1,0792 \right] \quad (5)$$

Where:

$$r = \sqrt{1,6 \cdot a^2 + h^2} - 0,675 \cdot h \quad (6)$$

- μ = Poisson's coefficient (0,2)
- E_{cm} = Secant Longitudinal Strain Modulus
- K = Ballast coefficient
- h = Screed thickness
- Maximum tensile stress on concrete on the underside of the slab due to a load applied at the edge:

$$\sigma_i = 0,275 \cdot (1 + \mu) \cdot \frac{P}{h^2} \cdot \left[\log \left(\frac{E_{cm} \cdot h^3}{k \cdot r^4} \right) - 54,54 \cdot \left(\frac{l}{5 \cdot l} \right)^2 \cdot 0,2 \right] \quad (7)$$

On the other hand, Meyerhof's analytical approach to determining the loads applied in internal, edge or corner areas is included in the *Technical Report 34 standard. Concrete Industrial Ground Floors* (Concrete Society, 2014).

Interpolating the a/l values between 0 and 0.2

For an internal load:

$$a/l = 0 \quad P_{u,0} = 2\pi(M_p + M_n) \quad (8)$$

$$a/l \geq 0,2 \quad P_{u,0,2} = 4\pi(M_p + M_n)/[1 - (a/3l)] \quad (9)$$

For edge loads:

$$a/l = 0 \quad P_{u,0} = [\pi(M_p + M_n)/2] + 2M_n \quad (10)$$

$$a/l \geq 0,2 \quad P_{u,0,2} = [\pi(M_p + M_n) + 4M_n]/\left[1 - \frac{2a}{3l}\right] \quad (11)$$

For corner loads:

$$a/l = 0 \quad P_{u,0} = 2M_n \quad (12)$$

$$a/l \geq 0,2 \quad P_{u,0,2} = 4M_n/[1 - (a/l)] \quad (13)$$

Where:

- M_n = negative resistance moment of the slab (kNm) understood as of simple unreinforced concrete (see section 6.3 TR34)
- M_p = last positive resistive moment of the slab (kNm) taking with that of reinforced concrete.

As indicated in the standard, equation (15) below only applies to reinforced slabs. For slabs only reinforced near the surface, it does not apply and must be considered as non-reinforced. For this reason, we can simplify the above expressions by considering $M_p = 0$: $M_{un} = M_n + M_p$

Maximum Moment:

$$M_{un} = f_{ctd,fl} \left(\frac{h^2}{6} \right) \quad (14)$$

$f_{ctd,fl}$ = Designed flexural strength

Reinforced Concrete Moment (M_p):

$$M_{pfab} = 0,95A_s f_{yk} d / \gamma_m \quad (15)$$

Where:

- A_s = Steel Area
- f_{yk} = Characteristic Strength of Steel
- d = Effective Productivity

III. RESULTS

Table 4 shows the ballast coefficients in (MN/m^3) obtained for each of the soils used in the calculations.

A. Toyota 8FBE20 Electric Counterbalance

Fig. 6 shows the influence of the hardness of the soil is relatively small with respect to the stresses in the concrete. The thickness of the screed is more decisive, reducing the influence of the thickness of the screed from thicknesses greater than 20 cm.

To check the influence of the type of concrete, the same check has been conducted for an HM30 concrete, being able to conclude that the stresses do not vary considerably for this type of loads, being again the most determining factor the thickness of the screed.

The following figures show the verification or non-verification of both Westergaard's and Meyerhof's equations. To be able to make a certain comparison between the two methods, following the TR-24 4th edition, in the case of Meyerhof, the flexural strength has been reduced between $Y_{M=1.5}$ and the load must be increased by $YG = 1.5$. This fact, being the most recent specification, leads to the adoption of a valid coefficient for Westergaard of 2.25 and 1 (% exceeded), once these operations have been conducted, with Meyerhof, this method being the one currently adopted and which serves as a reference. It is important to remember that Meyerhof is based on the method of exhaustion break lines, while Westergaard is a pseudo-empirical elastic procedure.

As shown in the following figures, for the load applied by the 8TBE20 stevedoring forklift, an HM25 concrete is verified in each of the five soil cases from screed thicknesses of 25 cm or more. In the case of using HM30 concrete, this thickness could be reduced by up to 20 cm, but only with soils with a ballast coefficient higher than those considered softer. In the case of Meyerhof, it would be verified for HM25 concrete with screed thicknesses of 20 cm or more and with HM30 concrete this value could be reduced to 15 cm.

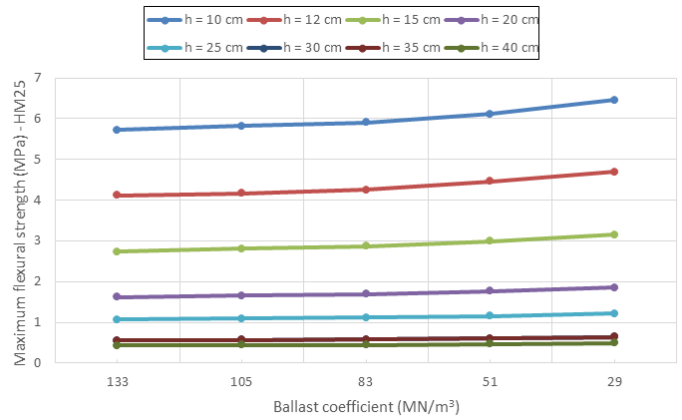


Fig. 6. Influence of the ballast coefficient on the maximum stresses in the slab. HM25 (Own elaboration)

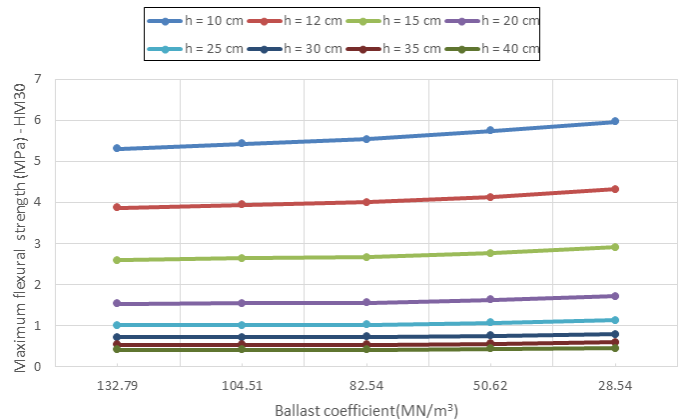


Fig. 7. Influence of the ballast coefficient on the maximum stresses in the slab. HM30 (Own elaboration)

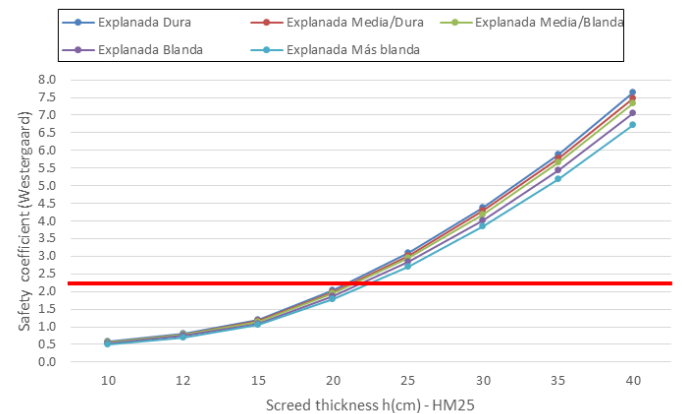


Fig. 8. Westergaard safety coefficient in HM25 screed (Own elaboration)

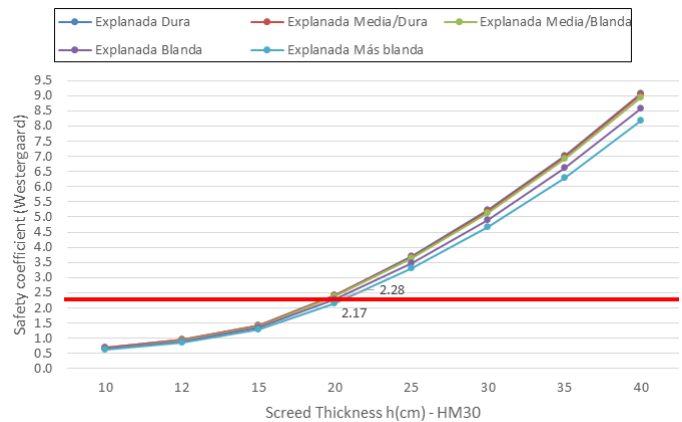


Fig. 9. Westergaard safety coefficient in HM30 screed (Own elaboration)

Soil	Ballast coefficient k_s (MN/m^3)
Hard ground soil (natural gravel)	133
Medium soil (hard sands, consolidated clays)	105
Medium soil (soft sands, semi-consolidated clays)	83
Soft Soil	51
Softer soils	29

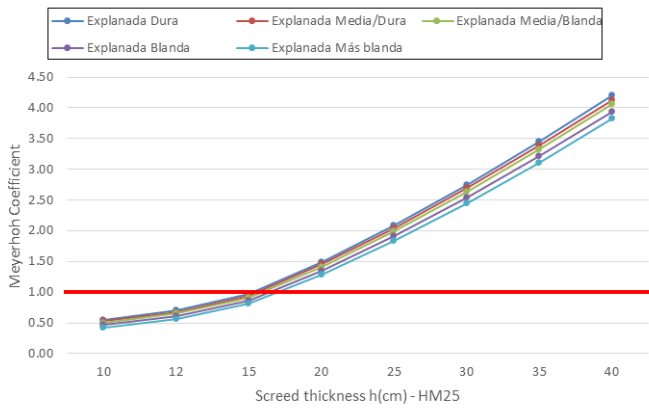


Fig. 10. Meyerhof exceedance coefficient in HM25 screed (Own elaboration)

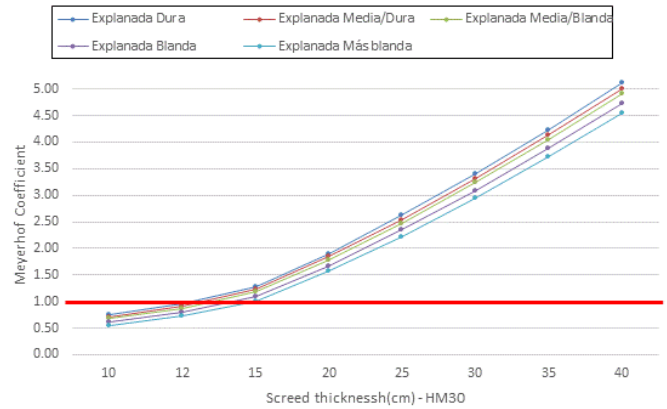


Fig. 11. Meyerhof exceedance coefficient in HM30 screed (Own elaboration)

B. Toyota 8FBE16 Electric Counterbalance

For the load applied by the Toyota 8FBE16 truck, it is verified with thicknesses from 20 cm and soils from medium/soft with HM25 concretes and verified for all types of

soil studied from 20 cm with HM30 concrete.

In the case of Meyerhof, for HM25 from soft soils and a thickness of 15 cm from screeds, this value would already be verified, reducing this value for HM30 to 12 cm from soft soils.

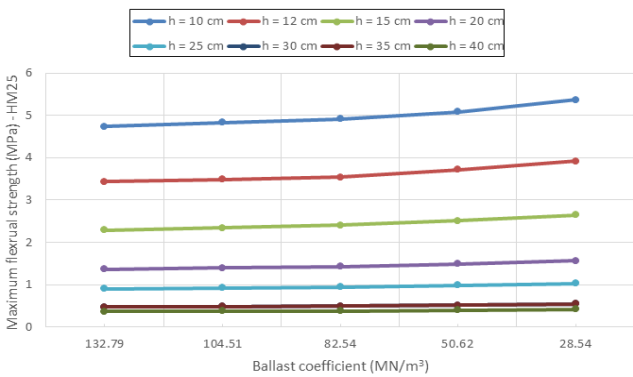


Fig. 12. Influence of the ballast coefficient on the maximum stresses in the slab. HM25 (Own elaboration)

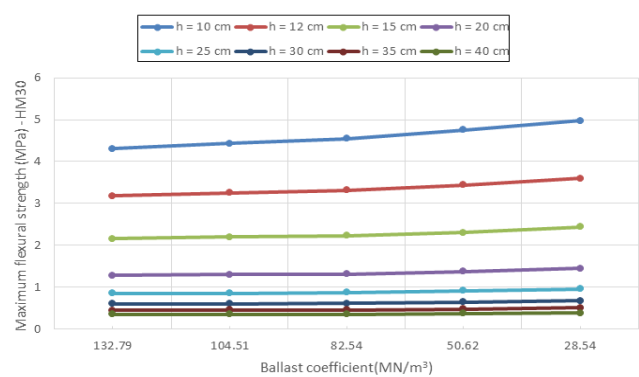


Fig. 13. Influence of the ballast coefficient on the maximum stresses in the slab. HM30 (Own elaboration)

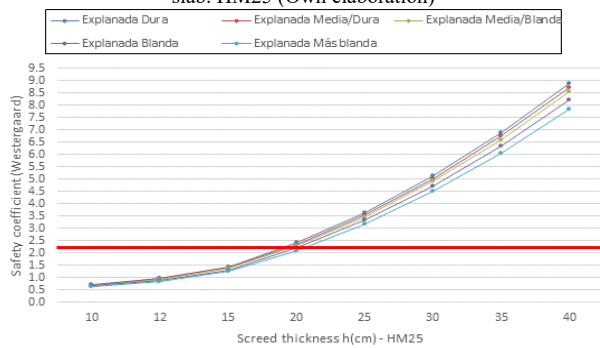


Fig. 14. Westergaard safety coefficient in HM25 screed (Own elaboration)

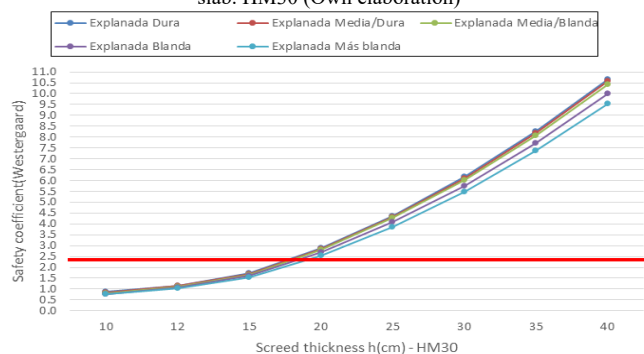


Fig. 15. Westergaard safety coefficient in HM30 screed (Own elaboration)

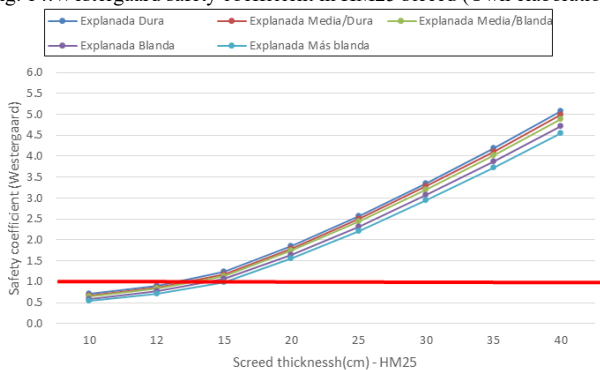


Fig. 16. Meyerhof exceedance coefficient in HM25 screed (Own elaboration)

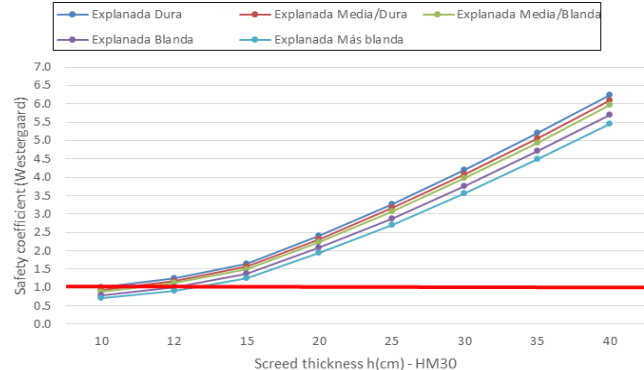


Fig. 17. Meyerhof exceedance coefficient in HM30 screed (Own elaboration)

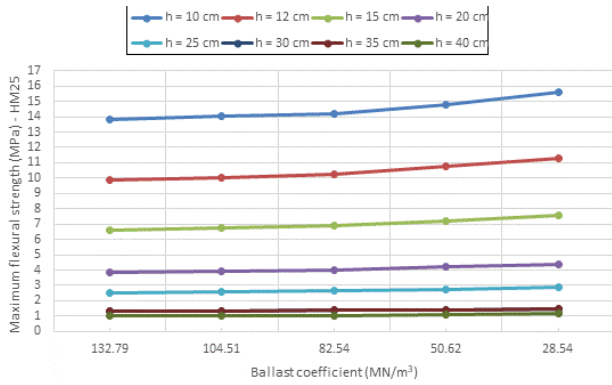


Fig. 18. Influence of the ballast coefficient on the maximum stresses in the slab. HM25 (Own elaboration)

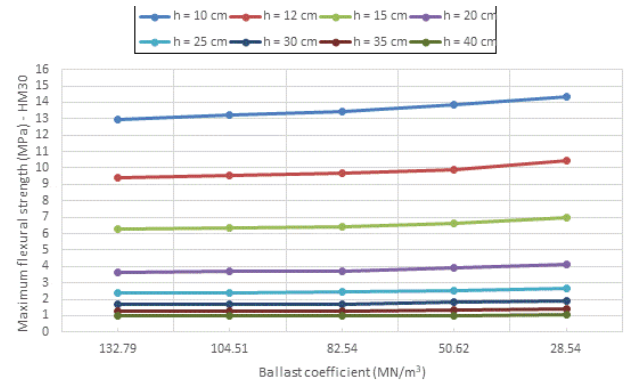


Fig. 19. Influence of the ballast coefficient on the maximum stresses in the slab. HM30 (Own elaboration)

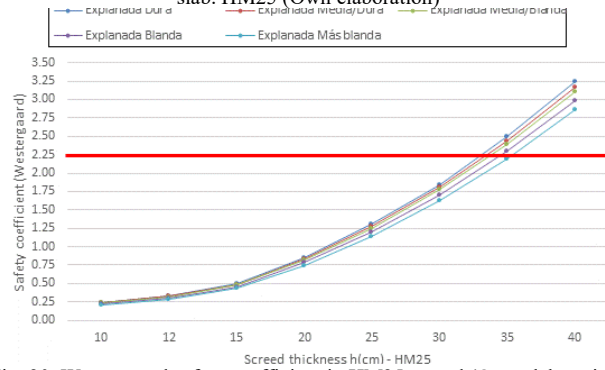


Fig. 20. Westergaard safety coefficient in HM25 screed (Own elaboration)

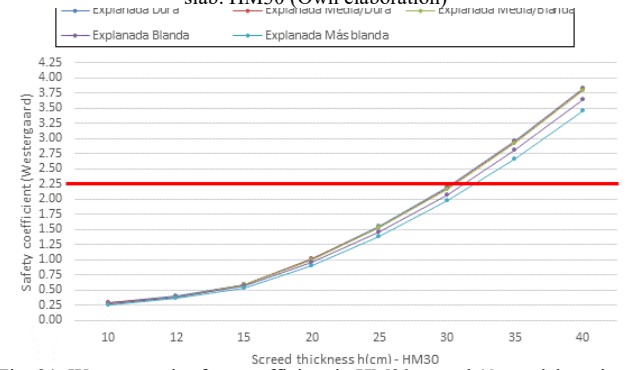


Fig. 21. Westergaard safety coefficient in HM30 screed (Own elaboration)

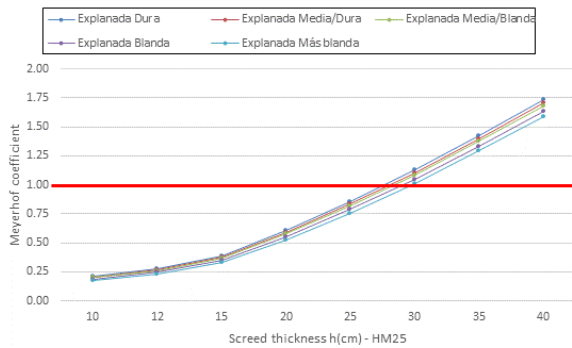


Fig. 22. Meyerhof exceedance coefficient in HM25 screed (Own elaboration)

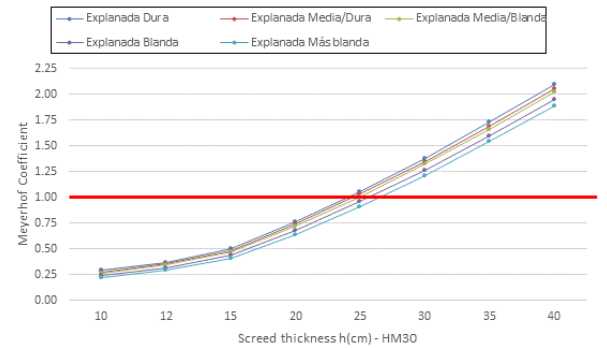


Fig. 23. Meyerhof exceedance coefficient in HM30 screed (Own elaboration)

C. Material racking in logistics centre.

As the load increases, although the thickness of the screed continues to be the most determining factor, the difference between concretes becomes more relevant.

For the load applied by the racking, it is verified with thicknesses from 35 cm and soft esplanades with HM25 concretes and verified for all types of esplanade studied from 35 cm with HM30 concrete.

In the case of Meyerhof, for HM25 from 30 cm of floor, this value for HM30 is reduced to 25 cm from medium/soft esplanades.

IV. CONCLUSIONS

We could conclude that, in fruit and vegetable plants, for areas where the most important load is the movement of goods with stevedoring forklifts, it would be appropriate to use a screed thickness of 20 cm or more for HM25 or 15 cm for HM30, verifying these for Meyerhof.

In the case of storage areas for goods, whether fruit or shelf

clothing material, this thickness should be increased to 30 cm for HM25 concrete or slightly lower, 25 cm for HM30 concrete and from medium/soft esplanades (ballast coefficient ≥ 83 MN/m³). In the case of using smaller thicknesses, it can lead to the progressive collapse of the screed, and it is quite common to wear racks for levelling in fruit and vegetable warehouses of a certain age (see Fig. 24).



Fig. 24. Detail of shelving in driveway cold room

REFERENCES

- CONCRETE SOCIETY. Concrete Industrial Ground Floors: A Guide to Their Design and Construction. Concrete Society, 1994. Pág.141
- CONCRETE SOCIETY. Concrete Industrial Ground Floors: A Guide to Their Design and Construction. Concrete Society, 2014.
- J.L. Escario, V. Escario, E. Balaguer (1973). Caminos (Tomo II) Firmes de carreteras y aeropuertos, p. 982. ETSI, Caminos, Canales y Puertos, Universidad Politécnica de Madrid
- FERRER, Carlos; FERRÁN, J. Javier; FERRER, Carlos. Contribución al estudio, cálculo y diseño de soleras de hormigón en masa para la actividad agroindustrial. Informes de la Construcción, 2000, vol. 51, no 466, p. 22-33.
- Gargallo Tatay, E., Ferrer Gisbert, C. M., Redón Santafé, M., FerrerR Gisbertt, P. S., & Ferrán Gozávez, J. J. (2022). Estudio de las acciones exteriores sobre soleras de hormigón en centrales hortofrutícolas.
- P. Juhasz Karoly, P.Schaul. Design of industrial floors-review of guidelines, special designing issues (part 1). Journal of Civil Engineering and Architecture, 2019, vol. 13, p. 330-336.
- P. Juhasz Karoly, P.Schaul. Design of Industrial Floors—TR34 and Finite Element Analysis (Part 2). J. Civ. Eng. Archit, 2019, vol. 13, p. 512-522.
- A. Martini, G. Bonelli, A. Rivola. Virtual testing of counterbalance forklift trucks: Implementation and experimental validation of a numerical multibody model. Machines, 2020, vol. 8, no 2, p. 26.
- NILSON, A.; WINTER, G. Diseño de estructuras de concreto. McGrawHill. 1994. Cap.14SERYKH, I. R.; CHERNYSHEVA, E. V.; DEGTYAR, A. N. Assessment load capacity in floor constructions. En IOP Conference Series: Materials Science and Engineering. IOP Publishing, 2019. p. 022001.
- K. Urbonas, D. Slizytė, A. Sapalas. The engineering method for unifying ground floor slab settlements. Engineering structures and technologies, 2020, vol. 12, no 2, p. 46-52
- Z. Tursikis et al. A novel integrated approach to solve industrial ground floor design problems. Sustainability, 2020, vol. 12, no 12, p. 4809.



Reconocimiento – NoComercial (by-nc): Se permite la generación de obras derivadas siempre que no se haga un uso comercial. Tampoco se puede utilizar la obra original con finalidades comerciales.